J. Fluid Mech. (1974), *vol.* 66, *part* 2, *pp.* 289–308
Printed in Great Britain

Electrohydrostatic instability in electrically stressed dielectric fluids. Part 1

By D. H. MICHAEL, J. NORBURY AND M. E. O'NEILL

Department of Mathematics, University College London

(Received 9 November 1973)

A theoretical investigation is presented of the electrohydrostatic stability of a given volume of incompressible dielectric fluid when stressed by the application of a potential difference between bounding conducting fluids. It is assumed that the dielectric fluid is located in a channel of breadth $2a$ and height $2h$, with $h/a \ll 1$, whose walls are semi-infinite solid dielectric sheets of thickness $2h$. The dielectric fluid may have a volume which differs from that of the channel, so that the presence of menisci at the interfaces between conducting and non-conducting fluids is taken into account. By a suitable method for approximating the electric stress at the interfaces, the electrostatic potential difference across the dielectric is determined as a function of the pressure difference across the interfaces for prescribed values of the discrepancy of the volume of the dielectric from the volume of the channel per unit length, and criteria are obtained for determining the critical electric field which precipitates the instability of the system. The variation of the critical electric field with the dimensionless volume excess 2δ is also found and it is shown that, for $\delta < -0{\cdot}5$, instability is associated with a symmetric mode of disturbance in which the critical field occurs at the maximum in a plot of potential difference *vs.* pressure difference. For $\delta > -0{\cdot}5$, instability arises from an asymmetric disturbance with the critical field occurring at a bifurcation point in the potential difference/pressure difference plane. Bifurcations are shown to occur only when the equilibrium profiles of the interfaces have extrema at the edges of the channel.

1. Introduction

The failure of the insulation of a dielectric fluid between electrified bodies, due to the mechanical instability of the fluid produced by the electrical stresses, has recently been the subject of a number of studies. Taylor & McEwan (1965) demonstrated such effects, produced under the influence of gravity by an electrified plate placed above a horizontal conducting free surface. Taylor (1968) gave an experimental and theoretical study of the instability of neighbouring soap film membranes when mounted on two circular rings, and Ackerberg (1969) undertook further mathematical analysis of this problem as formulated by Taylor. In experiments to verify the linear theory of waves on a conducting cylindrical column Taylor (1969) studied the bursting of a cylindrical membrane when stressed by a radial electric field. Studies of the waves on an electrified

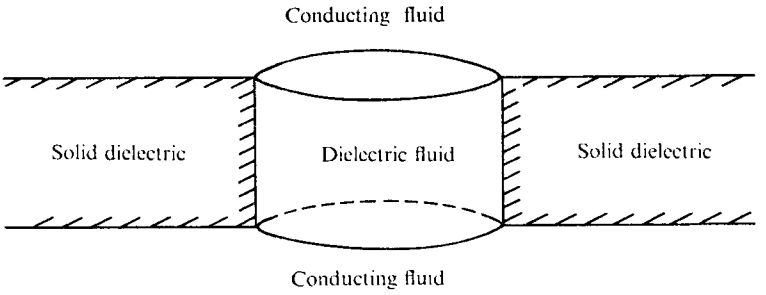

FIGURE 1. Schematic diagram of Zuercher's experiments.

conducting jet have been made by many authors, such as Bassett (1894), Rayleigh (1879), Melcher (1963) and Crowley (1965). The application of the theory of such waves to the instability of the cylindrical membrane in Taylor's experiments was made by Taylor (1969) and Michael & O'Neill (1972*a*), and good agreement with experimental results was obtained. Two-dimensional studies of the instability of neighbouring electrified conducting surfaces were given by Michael & O'Neill (1972*b*).

The motivation and starting point for the further study presented in this paper is the investigation of Michael, O'Neill & Zuercher (1971), hereafter referred to as MONZ, in which an experimental and theoretical study was made of the breakdown of the insulation of a fluid dielectric contained in a circular hole in a sheet of solid dielectric. The geometry of these experiments conducted by Zuercher is reproduced in figure 1. A right circular hole in a Perspex plate was filled with a dielectric fluid and was enclosed above and below by two layers of water across which a potential difference was applied. The dielectric fluid in the hole was made neutrally buoyant so that the effect of gravity did not enter the problem. Observations of the potential difference at which the fluid insulation becomes unstable were made for a number of holes of different radius-to-depth ratio. Agreement between the results of these experiments and the mathematical analysis was good, but small discrepancies in the results could be explained by the difficulty in controlling exactly the conditions of the experiment. In particular, it was difficult to ensure that the volume of dielectric fluid used was exactly the right amount to fill the hole and it was suggested that small divergences between observational results and theoretical predictions could be accounted for by small discrepancies in the volume of fluid filling the hole. These considerations have prompted the present authors to consider whether the mathematical analysis given in MONZ can be advanced to include calculations of the instability when the hole is not exactly filled.

In the absence of any gravitational effects, when the hole is underfilled or overfilled the upper and lower surfaces will be symmetric about the centre-plane, and when there is no applied field they will evidently be spherical if the effect of the menisci is taken into account. When an electric field is applied across the hole it becomes a matter of considerable difficulty to calculate the shape of the interfaces. Such a specification can be given in general only in numerical terms, and, if the problem is conceived in this way, it follows that calculation of the instability

can be effected only in numerical form. However, the problem can be advanced theoretically in a more satisfactory way when the hole radius is large in relation to its depth by making use of the approximation given by Taylor (1968) in his study of the instability of electrified soap films suspended on two similarly situated circular rings. Denoting the distance between the rings by $2h$, the radius of the rings by a, and the radius of curvature of the membranes in the absence of an electric field by R, Taylor considered the situation in which $h \ll a \ll R$, and he demonstrated that very good agreement with experiment can be obtained by approximating the field strength by the field between parallel planes separated by the local separation of the membranes. This formulation leads to the two-point boundary-value problem in which the profile of the membrane satisfies the equations

$$\left.\begin{aligned} \frac{d^2y}{dx^2}+\frac{1}{x}\frac{dy}{dx} &= \alpha+\frac{\beta}{y^2} \quad (y \geqslant 0), \\ dy/dx = 0 \quad (x = 0), \quad y &= 1 \quad (x = 1). \end{aligned}\right\} \tag{1}$$

Here x is made dimensionless on the scale a, y is dimensionless on the scale h, and $\alpha = 2a^2/Rh$ and $\beta = KV_0^2a^2/16\pi Th^3$ are two constants which represent, in dimensionless form, respectively, the defect in the static pressure in between the two membranes compared with the pressure outside, and the level of the potential difference $2V_0$ applied between the membranes. T is the one-sided surface tension and K the dielectric constant of the medium between the membranes.

We may apply the formulation (1) also to Zuercher's experiments when the hole radius is large compared with the depth if we replace T by $\frac{1}{2}T$ since the surfaces under stress are not now membranes, but the form of solution in this case is different. In Taylor's work it was assumed that a change in the equilibrium configuration of the membranes occurs with the application of the field under conditions in which the pressure difference, measured by α, remains invariant. The obvious instance of this is when the rings are open-sided, with $\alpha = 0$, which was the condition of Taylor's experiments. Thus solutions of (1) were sought by Taylor and Ackerberg at constant α, and transition to instability was found at a maximum value of β subject to this condition. When an incompressible dielectric fluid fills a circular hole with closed sides, the solution of the mathematical problem (1) must take a different form. Clearly in this case the change in the equilibrium configuration with the application of an electric field must be accompanied by a change in pressure in such a way that the volume of fluid occupying the hole remains constant. The requirement in this case is therefore to obtain solutions of (1) in which α and β vary in such a way as to maintain the volume of fluid constant. The most convenient way of representing such solutions is to plot the locus of (α, β) in the α, β plane for each prescribed volume fraction.

It may be noted here that constant-volume conditions are not confined to liquid insulators. In the experiments of Taylor (1969), for example, it was demonstrated that the bursting by electrification of a cylindrical membrane enclosing an air column which is closed at the ends takes place through incompressible modes of instability. In such cases the level of the surface stresses produced by electrification in the critical state is too low to have any appreciable effect in expanding or

compressing the enclosed air. Thus a simple counterpart of the conditions of Zuercher's experiments could be realized by an arrangement in which a box is constructed with insulating sides and conducting plane surfaces above and below in which two circular holes are made centrally. With two soap film membranes spread over the holes to enclose the air in the box and a means of setting the pressure inside to vary the volume of air in the box, the conditions of Zuercher's experiment can be simulated.

In seeking to connect the results of an analysis of this kind with the results of the small perturbation analysis in MONZ several points need elucidation. In the first place the analysis in MONZ was given in two parts, an approximate and an exact theory, the approximate theory being one in which the conditions at the side of the hole are not exactly satisfied. The difference between the results of these two theories diminishes as the hole radius gets larger. It is to be expected that the Taylor analysis will be valid in the limit of very large holes, and it is therefore appropriate to make comparisons with the results of the approximate theory, which are given in a simple explicit form. A second point arising in the comparison is that in MONZ two forms of unstable modes were shown to be relevant, sausage and kink modes, these being respectively small perturbations of the hole surface symmetric and antisymmetric about the centre-plane. The Taylor formulation has been given only for sausage-type equilibria which are also symmetric about the axis of the hole. It may be asked whether there is any counterpart to kink modes in the Taylor formulation. Such modes imply equilibria which are not symmetric about the centre-plane and it can easily be seen that they cannot occur. For, if we denote the two surfaces, which may now be of arbitrary (axisymmetric) shape, by $y_1(x)$ and $y_2(x)$ the equations for axisymmetric equilibria may be written as

$$\frac{d^2y_2}{dx^2}+\frac{1}{x}\frac{dy_2}{dx}=\alpha+\frac{4\beta}{(y_2-y_1)^2},$$

$$\frac{d^2y_1}{dx^2}+\frac{1}{x}\frac{dy_1}{dx}=-\alpha-\frac{4\beta}{(y_2-y_1)^2},$$

with

$$dy_1/dx = dy_2/dx = 0 \quad \text{at} \quad x = 0; \qquad y_1 = 0, \quad y_2 = 2 \quad \text{at} \quad x = 1.$$

If $\xi = y_1+y_2$ and $\eta = y_2-y_1$, it follows, by adding the equations, that $\xi = 2h$, and hence that $y_1 = h-\frac{1}{2}\eta$ and $y_2 = h+\frac{1}{2}\eta$. Therefore no kink-type solutions symmetric about the axis will exist. The result is unaltered for modes which are not axisymmetric, because in this case we require ξ to satisfy Laplace's equation

$$\frac{\partial^2\xi}{\partial x^2}+\frac{1}{x}\frac{\partial\xi}{\partial x}+\frac{1}{x^2}\frac{\partial^2\xi}{\partial\theta^2}=0,$$

with $\xi = 2h$ at $x = 1$ for all values of the polar angle θ. Hence again $\xi \equiv 2h$. Thus the Taylor form of analysis can only be associated with sausage mode displacements because the electrical stress at corresponding points on the upper and lower surfaces is the same, so that the curvature of the surfaces must have the same value with opposite sign at these points. This is compatible with the sausage modes of MONZ, where the normal field is even about the mid-plane,

giving equal stresses on both surfaces, whereas in the kink modes the values of the perturbation normal stresses at the two surfaces are equal and opposite, giving different first-order stresses at the two surfaces. This connexion between the two theories is also confirmed by the form of the dispersion relationship for neutrally stable waves given in MONZ. It was shown that the relationship is

$$KE_0^2 = 4\pi kT \tanh Rh, \quad \text{for sausage modes,} \tag{2a}$$

$$KE_0^2 = 4\pi kT \coth Rh, \quad \text{for kink modes,} \tag{2b}$$

where $E_0 = V_0/h$ is the unperturbed field strength and k is the wavenumber. The Taylor analysis corresponds to the case where $kh \to 0$, when $(2a)$ gives rise to a finite limit k^2a^2 for $2\beta = KV_0^2a^2/4\pi Th^3$. (In MONZ the symbol R was used instead of a and it was seen that kR could take finite and discrete values.) In $(2b)$ it is easily seen that there is no finite limit for β.

The primary interest in both forms of the theory is to find the mode of breakdown which has the lowest level of applied potential V_0. In the MONZ analysis of a fully filled hole it was shown that for small holes this mode is an axisymmetric kink mode, and for a large hole it is a non-axisymmetric sausage mode. From the foregoing discussion we should expect to be able to apply the Taylor form of analysis to obtain the lowest mode for partially filled large holes, but a complication arises because by implication from the MONZ result it is to be expected that this will be a non-axisymmetric mode. The equations for non-axisymmetric equilibrium using the Taylor formulation will give rise to the boundary-value problem, which follows by extension from (1);

$$\left.\begin{aligned} &\frac{\partial^2 y}{\partial x^2} + \frac{1}{x}\frac{\partial y}{\partial x} + \frac{1}{x^2}\frac{\partial^2 y}{\partial \theta^2} = \alpha + \frac{\beta}{y^2} \quad (y \geqslant 0), \\ \text{with} \quad &y = 1 \quad \text{when} \quad x = 1 \quad \text{for} \quad 0 \leqslant \theta < 2\pi. \end{aligned}\right\} \tag{3}$$

Non-axisymmetric solutions of this boundary-value problem are difficult to obtain, and in order to examine the connexion between axisymmetric and non-axisymmetric solutions in a slightly easier context, it was decided to make a study in the first place of the corresponding two-dimensional problem in which the hole becomes a rectangular channel. This problem has the advantage of not introducing a second independent variable for asymmetric modes. Also, the counterpart of the Taylor theory for constant α in the two-dimensional problem has already been given by Michael & O'Neill (1972*b*), and it has the further advantage of giving solutions in terms of tabulated elliptic integrals.

Our discussion of the problem will therefore be presented in two parts. The first part, which takes up the remainder of this paper, gives a complete account of the counterparts of the MONZ and Taylor theories in the two-dimensional case, where a comprehensive analytical approach to the problem allows the connexion between the two theories for large holes filled with incompressible non-conducting fluid to be made clear. In a second paper we shall give an account of the results which are obtainable for a circular hole using the Taylor theory and the connexion between these results and those of the theory given previously in MONZ. Here, for the most part, a numerical study of the problem has had to be carried out.

2. Small perturbation theory for a two-dimensional hole

We begin our analysis of the breakdown of stability in a two-dimensional hole by formulating the counterpart of the linear theory given in MONZ for a circular hole.

Insulating fluid now fills an infinitely long channel of depth $2h$ and width $2a$ bounded by semi-infinite sheets of solid dielectric. There are plane interfaces at $y = \pm h$, $|x| \leqslant a$, between the insulating fluid and conducting fluid above and below the sheets. If $\zeta(x)$ denotes the y displacement of the interface for neutrally stable small two-dimensional disturbances, we distinguish between sausage and kink modes, in which $\zeta(h) = -\zeta(-h)$ and $\zeta(h) = +\zeta(-h)$ respectively. It is assumed that the edges of the channel $|x| = a$, $y = \pm h$ are sharp. In this case with the insulating fluid wetting the sides of the channel up to the edges, the fluid surface will be suspended from the sharp edges at an angle of inclination which may take any value depending on the volume of the insulating fluid. Thus $\zeta = 0$ at the two ends of the interfaces at $x = \pm a$. As a counterpart of axisymmetric and non-axisymmetric modes for a circular hole we also distinguish between modes in which ζ is symmetric or antisymmetric about the y axis. For antisymmetric modes $\zeta_n \propto \sin k_n x$, where $k_n = n\pi/a$, $n = 1, 2, 3, \ldots$, and for symmetric modes $\zeta_n \propto \cos k_n x$, with $k_n = (n + \frac{1}{2})\pi/a$. The electrostatic potential ψ of the perturbation satisfies Laplace's equation and the boundary conditions $\chi + E_0\zeta = 0$ at $y = \pm h$, where E_0 is the applied field in the y direction across the hole. In a simplified theory, in which χ is made zero at $|x| = a$, the field in the hole is not coupled to the field outside it, and for anti-symmetric sausage modes, χ will have the form χ_n, where

$$\chi_n = A_n \sinh k_n y \sin k_n x,$$

with

$$A_n = -E_0\zeta_n / \sinh k_n h.$$

The normal stress condition at $y = h$ then gives

$$T\frac{d^2\zeta}{dx^2} = \frac{KE_0}{4\pi}\frac{\partial\chi}{\partial y},$$

so that

$$KE_0^2 h/4\pi T = k_n h \tanh k_n h, \tag{4}$$

where K is the dielectric constant of the fluid in the hole and T is the surface tension. The lowest field strength E_0 which will give instability is given from (4) by the lowest value of k_n, i.e. $k_1 = \pi/a$; this we shall refer to as the $S1$ mode. In the case of kink modes, in which χ is an even function of y, the dispersion relation corresponding to (4) is now

$$KE_0^2 h/4\pi T = k_n h \coth k_n h. \tag{5}$$

For a given value of k_n, the sausage mode instability always appears at a lower value of E_0, but the symmetric sausage modes cannot appear because they each result in a change in the volume of fluid filling the hole. Hence $S1$ is the first sausage mode of instability. Symmetric kink modes can occur with $k_n = (n + \frac{1}{2})\pi/a$, and the lowest kink mode, which we denote by $K0$, is obtained from (5) with $k_0 = \pi/2a$. For small h/a, the sausage mode $S1$ becomes unstable

first with increasing E_0, while for large h/a, the kink mode $K0$ is the most unstable. The transition in unstable modes occurs when $h/a \approx 0{\cdot}5$.

These conclusions are based on the assumption that, in the state of marginal stability, no change in static pressure inside the fluid dielectric occurs relative to the outer conducting fluids. It is of interest to note in connexion with the Taylor approximations given later that a relaxation of this condition can give rise to a form of symmetric sausage mode. An account of such modes for a circular hole is given by Michael & O'Neill in an appendix to part 2 of this work. In the plane geometry an approximate representation of such a symmetric mode may be obtained by writing $\zeta = A(\cos kx - \cos ka)$, where A is a small amplitude. This will satisfy the condition $\zeta = 0$ at $|x| = a$. The constant-volume condition necessary for a sausage mode, which is

$$\int_0^a \zeta \, dx = 0,$$

requires that $\tan ka = ka$. The lowest value of k occurs when $ka = 4{\cdot}49$. For such a mode we have an electrostatic potential of the form

$$\chi = -A\left\{E_0 \frac{\sinh ky}{\sinh kh} \cos kx - E_0 \frac{y}{h} \cos ka\right\}, \tag{6}$$

and it may be seen that the extra term in (6) gives rise to an extra constant term in the first-order electric stress at $y = h$, which is now

$$\frac{KE_0^2}{4\pi} A\left\{k \coth kh \cos kx - \frac{\cos ka}{h}\right\}.$$

The dispersion relation (4) follows as previously, using the first term. The second term illustrates that such a mode can arise only when there is a small first-order increase δp in the static pressure inside the channel, this being given by

$$\delta p = -(KE_0^2 A/4\pi h) \cos ka. \tag{7}$$

The critical value of E_0 predicted by this approximation is given by (4) with $ka = 4{\cdot}49$. For a given channel, this is higher than the value for an $S1$ mode, in which $ka = \pi$. Provided that these represent good approximations, this symmetric sausage mode should not enter into any correlation of theory with experimental observations of instability. A reservation concerning this mode is that from (6) it does not satisfy the condition $\chi = 0$ at $|x| = a$, $|y| < h$ as do previous modes. However, in the limiting case $kh \to 0$, which connects up with the Taylor approximation, this condition is then satisfied.

We can also consider an approximation to a kink mode with this form of ζ, in this case without restriction on the value of k. The potential χ now has the form

$$\chi = -AE_0\left\{\cos kx \frac{\cosh ky}{\cosh kh} - \cos ka\right\}.$$

The additional term in χ is a constant, and gives no additional stress, no change in static pressure and no change in the dispersion relation. Again, this form of solution does not make $\chi = 0$ when $|x| = a$, $|y| < h$, except in the limit $kh \to 0$.

In so far as both these approximate solutions are unable to satisfy continuity conditions at the sides $|x| = a$, $|y| < h$, they cannot be expected to give accurate values for the critical field E_0. But they are of value in showing that changes in internal pressure are associated with symmetric sausage modes, but not with symmetric kink modes. A full solution for these modes incorporating continuity conditions at the sides has been given by Miss A. E. Latham (1973, private communication) and will not be pursued further here.

A final point concerning this form of analysis is that we have assumed a two-dimensional form of perturbation in which ζ and χ are independent of the co-ordinate z along the channel. It can easily be seen that a simple form of Squires' theorem applies in this case in the sense that, if ζ is taken to be of the form $\zeta = \frac{\sin}{\cos} kx \frac{\sin}{\cos} mz$, the critical field strengths are given by either (4) or (5) with k replaced by the larger value $(k^2+m^2)^{\frac{1}{2}}$. Since the critical values of E_0 increase with increasing k we conclude that a two-dimensional form of disturbance will yield the first point of instability. This is confirmed by the work of Miss A. E. Latham when $k/a \ll 1$. It has also been demonstrated both experimentally and theoretically that the two-dimensional axisymmetric disturbance is more unstable than a three-dimensional disturbance in the analogous problem of the bursting of a charged cylindrical film. The experimental work of Taylor (1969) and the subsequent theoretical work of Michael & O'Neill (1972*a*) show that, for long films, it is the two-dimensional varicose mode which first becomes unstable.

The analysis described in this section pertains only to the case of a fully filled channel, for which the volume excess $\delta = 0$. By continuity it is clear that when $\delta \neq 0$ the system will first become unstable through a two-dimensional disturbance if $|\delta|$ is sufficiently small. In fact it can be easily verified that this must also be the case for any δ when the conditions for the validity of the Taylor formulation of the problem, set out in the previous section, are met, since the first-order change in the surface-tension stress is then always of the form $T(\partial^2\zeta/\partial x^2 + \partial^2\zeta/\partial z^2)$ and the conclusion follows as in the case $\delta = 0$.

3. Sausage mode instability for large holes

In the case of a plane-channel hole it is now appropriate to write the boundary-value problem (3) as

$$\frac{\partial^2 y}{\partial x^2} + \frac{\partial^2 y}{\partial z^2} = \alpha + \frac{\beta}{y^2}, \quad y(x) \geqslant 0,$$

with $y = +1$ at $|x| = 1$ for all z. The small perturbation analysis of the previous section has shown that for a fully filled hole the most unstable displacements will be two-dimensional in the sense that they are independent of z. This will also be true for partially filled plane holes, in which case the problem reduces to a search for equilibria $y(x)$ satisfying the conditions

$$\left.\begin{aligned} d^2y/dx^2 &= \alpha + \beta/y^2 \quad (y \geqslant 0), \\ y &= 1 \quad \text{when} \quad |x| = 1. \end{aligned}\right\} \tag{8}$$

In this case $\alpha = a^2/hR$ and $\beta = KV_0^2a^2/8\pi Th^3$. This boundary-value problem has been studied previously by Michael & O'Neill (1972*b*), under the assumption that α is constant. Here we seek solutions in which the volume of fluid occupying the hole is constant. This we measure by defining the excess of fluid occupying the hole as 2δ, where

$$\delta = \int_{-1}^{+1} (y-1)\,dx$$

in dimensionless form. Equation (8) has the advantage compared with (1) of having elliptic integral solutions in tabulated form. It also has a first integral of the form $(dy/dx)^2 = f(y)$, which is of great advantage in yielding a simple criterion for the bifurcation of the solutions which enables us to ascertain points where the stability changes. Our primary objective in this work is to obtain the locus of points in the α, β plane for which solutions of (8) have a prescribed value of δ.

For the purposes of numerical calculation it is useful to remove one of the parameters from (8).

If $\alpha > 0$, we write $\gamma = \beta/\alpha > 0$ and $x_1 = \alpha^{\frac{1}{2}}x$. Dropping the suffix we then have

$$d^2y/dx^2 = 1+\gamma/y^2, \quad \text{with} \quad y = 1 \quad \text{at} \quad |x| = \alpha^{\frac{1}{2}}.$$

A first integral is $\frac{1}{2}(dy/dx)^2 = \kappa + y - \gamma/y$, where κ is a constant. Real solutions of the boundary-value problem must have $dy/dx = 0$ at least once in the interval. Here $dy/dx = 0$ where $y^2+\kappa y-\gamma = 0$, which we write as $(y-b)(y-c) = 0$, with $bc = -\gamma < 0$ and $b+c = -\kappa$. Taking $b > 0$, the solutions thus have a single minimum when $y = b$ for $|x| \leqslant \alpha^{\frac{1}{2}}$. It also follows from the form of (8) that the solutions $y(x)$ are symmetric about the ordinate at a stationary point of $y(x)$. Thus, the minimum value of $y(x)$ must occur at $x = 0$ and consequently only solutions of (8) which are even functions of x are possible when $\alpha > 0$.

If $\alpha < 0$, we write $\gamma = -\beta/\alpha > 0$ and $x_1 = (-\alpha)^{\frac{1}{2}}x$. We now have

$$d^2y/dx^2 = -1+\gamma/y^2,$$

with $\frac{1}{2}(dy/dx)^2 = \kappa - y - \gamma/y = y^{-1}(b-y)(y-c)$. Now $b+c = \kappa$ and $bc = \gamma > 0$. Assuming $b > c$, it follows that $c \leqslant y(x) \leqslant b$, and solutions will have a maximum at $y = b$ and a minimum at $y = c$. Further, since $y(x) \geqslant 0$ in solutions of interest, and b and c have the same sign, we must have $b > c > 0$ in general. In this case it is clear that solutions with any number of alternate maxima and minima may be obtained.

As may be seen in later work described in this paper, the case $\alpha < 0$ is of most interest, and we continue the analysis for this case. We note that, since $dy/dx = \pm$ a function of y, it follows that the solutions $y(x)$ are periodic in x and since d^2y/dx^2 is a function of y^2, any solution is symmetric about all ordinates through the maxima and minima.

A basic half-wavelength $\frac{1}{2}\lambda$ of the solution occurs between $y = b$ and $y = c$, as shown in figure 2. With $y = 1$ at the ends of the range, clearly $b > 1 > c$, and three basic solutions are given by the abscissa ranges AB, BC and AC, the latter being one wavelength. The entire set of solutions can be obtained by adding an integral number of complete wavelengths to each of these three basic solutions. A distinction can be noted here between solutions which are symmetric (that is even

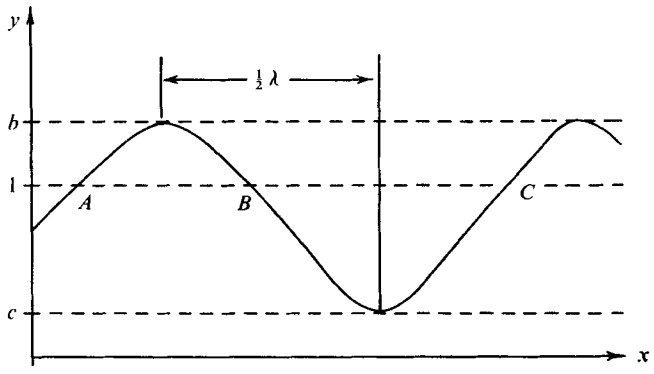

FIGURE 2. The solution of (8) when $\alpha < 0$. The basic interfacial profiles are AB or BC for solutions symmetric (even) in x and AC for asymmetric solutions.

functions of x about the centre-plane $x = 0$ of the hole), and those which are asymmetric in this sense. Evidently, solutions represented by the profiles AB, BC and all profiles obtained from these by adding an integral number of whole wavelengths to either will be symmetric profiles. Asymmetric profiles are represented by any integral number of whole wavelengths.

We also note that, whereas for symmetric profiles the slopes at the two ends are of the form $+m$ and $-m$, for asymmetric profiles they are equal. This leads to a simple criterion, of importance later, for the points at which asymmetric solutions bifurcate from symmetric solutions. If the bifurcation is smooth this clearly requires that the slope of the profile at each end shall be zero. The volume conservation condition is conveniently expressed in the form

$$\delta = \frac{1}{(-\alpha)^{\frac{1}{2}}} \int_{x=-(-\alpha)^{\frac{1}{2}}}^{+(-\alpha)^{\frac{1}{2}}} (y-1)\frac{dx}{dy}dy, \tag{9}$$

with dx/dy determined from the first integral of (8). This integral is in general an incomplete elliptic integral. But in the case of a complete wavelength solution AC it becomes a complete elliptic integral, and consequently,

$$\begin{aligned}\delta &= \frac{2}{(-\alpha)^{\frac{1}{2}}} \int_{y=c}^{y=b} \frac{(y-1)y^{\frac{1}{2}}dy}{\{2(b-y)(y-c)\}^{\frac{1}{2}}} \\ &= \frac{2(2b)^{\frac{1}{2}}}{3(-\alpha)^{\frac{1}{2}}}\left[(2b+2c-3)E\left(\frac{\pi}{2}, \left(\frac{b-c}{b}\right)^{\frac{1}{2}}\right) - cF\left(\frac{\pi}{2}, \left(\frac{b-c}{b}\right)^{\frac{1}{2}}\right)\right],\end{aligned} \tag{10}$$

where E and F denote respectively the elliptic integrals of the first and second kinds. We also have

$$\begin{aligned}2(-\alpha)^{\frac{1}{2}} &= \int_{x=-(-\alpha)^{\frac{1}{2}}}^{+(-\alpha)^{\frac{1}{2}}} \frac{dx}{dy}dy \\ &= \int_{x=-(-\alpha)^{\frac{1}{2}}}^{+(-\alpha)^{\frac{1}{2}}} \frac{y^{\frac{1}{2}}dy}{\{2(b-y)(y-c)\}^{\frac{1}{2}}}.\end{aligned} \tag{11}$$

For the whole wavelength solution AC this may also be written as a complete elliptic integral and takes the form

$$2(-\alpha)^{\frac{1}{2}} = 2(2b)^{\frac{1}{2}}E(\tfrac{1}{2}\pi, (1-c/b)^{\frac{1}{2}}). \tag{12}$$

For the whole wavelength solution the curves δ = constant in the α, β plane were obtained by the following procedure. Equation (10) may be rewritten, using (12) and considering δ as prescribed, as follows:

$$2b + 2c - 3 - \tfrac{3}{2}\delta = cF(\tfrac{1}{2}\pi, (1-c/b)^{\frac{1}{2}})/E(\tfrac{1}{2}\pi, (1-c/b)^{\frac{1}{2}}). \tag{13}$$

Values of $b \geqslant 1$ were set, and (13) was used, by interpolation from standard tables of complete elliptic integrals such as Abramovitz & Stegun (1965), to find corresponding values of c where $0 < c \leqslant 1$. Thereafter, equation (12) yields the value of α, and β is then obtained from the equation $\gamma = -\beta/\alpha = bc$. There is no solution when $b < 1$. In the limiting cases when $b = 1$, the solution AB of figure 2 ceases to exist and the solutions BC and AC coalesce. This represents the bifurcation of symmetric and asymmetric solutions, which can occur for $\delta < 0$, and for which $dy/dx = 0$ at the two ends of the range, as was remarked earlier. Also solutions can exist only when $c \leqslant 1$. Similar remarks apply to the limit in which $c = 1$, but clearly solutions will exist in this limit only for $\delta > 0$. This procedure enables us to obtain the whole wavelength loci, labelled λ, in figures 3, 5 and 6. A simple connexion exists between the solutions for one wavelength λ and those for any integral number of wavelengths. The solutions representing $n\lambda$, $n = 2, 3, 4, \ldots$, each require for fixed γ that the range of x be increased in the ratio n. Since this is represented by $|x| \leqslant (-\alpha)^{\frac{1}{2}}$ and the integral for δ is unchanged, it follows that α and β are increased in the ratio n^2. Hence, the loci for $2\lambda, 3\lambda, 4\lambda, \ldots$, follow from the λ loci by scaling up α and β in the ratios 4, 9, 16, ..., for any given δ. The symmetric loci, involving a non-integral number of wavelengths, are found by a similar procedure, using in this case tables of values of incomplete integrals such as Abramovitz & Stegun (1965). These calculations yield the loci labelled r, s, $\lambda + r$, $\lambda + s$, $2\lambda + r$, $2\lambda + s$, etc. in figures 3, 5 and 6, where as a convention for labelling the different solution profiles, we denote by r and s the profiles of the form AB and BC of figure 4. For the profile $n\lambda + r$ we reduce (9) and (11) to the following:

$$\delta = \frac{2}{3}\left(\frac{2}{-\alpha}\right)^{\frac{1}{2}} b^{\frac{1}{2}} \left\{(2b+2c-3)\left[nE\left(\frac{\pi}{2}, \left(\frac{b-c}{b}\right)^{\frac{1}{2}}\right) + E\left(\mu, \left(\frac{b-c}{b}\right)^{\frac{1}{2}}\right)\right]\right.$$
$$\left. - c\left[nF\left(\frac{\pi}{2}, \left(\frac{b-c}{b}\right)^{\frac{1}{2}}\right) + F\left(\mu, \left(\frac{b-c}{b}\right)^{\frac{1}{2}}\right)\right] + b^{-\frac{1}{2}}[(b-1)(1-c)]^{\frac{1}{2}}\right\},$$
$$2(-\alpha)^{\frac{1}{2}} = 2(2b)^{\frac{1}{2}}\left[nE\left(\frac{\pi}{2}, \left(\frac{b-c}{b}\right)^{\frac{1}{2}}\right) + E\left(\mu, \left(\frac{b-c}{b}\right)^{\frac{1}{2}}\right)\right],$$

where the argument μ of the elliptic integrals is given by $\sin^{-1}[(b-1)/(b-c)]^{\frac{1}{2}}$, and $n = 0, 1, 2, \ldots$. Corresponding equations for the profiles $n\lambda + s$ can be derived from the above by noting that $n\lambda + s = (n+1)\lambda - r$, for $n = 0, 1, 2, \ldots$. Again we consider δ as prescribed and consequently the above equations reduce to the following equation, which is analogous to (13):

$$(2b + 2c - 3 - \tfrac{3}{2}\delta)\left[nE\left(\frac{\pi}{2}, \left(\frac{b-c}{b}\right)^{\frac{1}{2}}\right) + E\left(\mu, \left(\frac{b-c}{b}\right)^{\frac{1}{2}}\right)\right]$$
$$= c\left[nF\left(\frac{\pi}{2}, \left(\frac{b-c}{b}\right)^{\frac{1}{2}}\right) + F\left(\mu, \left(\frac{b-c}{b}\right)^{\frac{1}{2}}\right)\right].$$

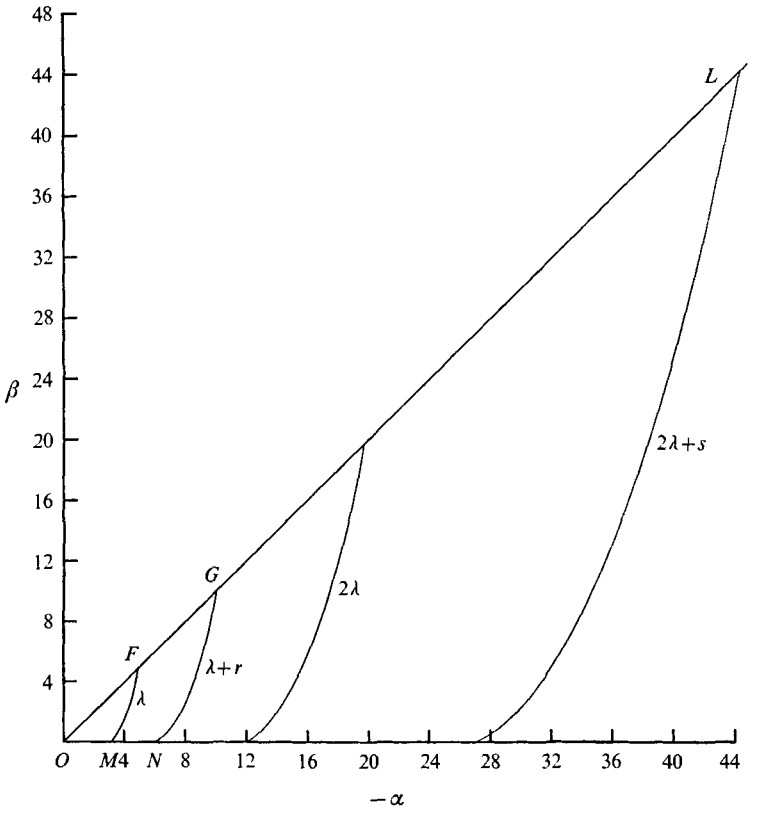

FIGURE 3. β *vs.* α for the solutions of (8) when $\delta = 0$. The label $n\lambda$ relates to a profile of n complete wavelengths, $n\lambda + r$ relates to a profile of type AB plus n complete wavelengths and $n\lambda + s$ relates to a profile of type BC plus n complete wavelengths.

We solve these equations by setting values of $b \geqslant 1$ and finding the corresponding values of c, where $0 < c \leqslant 1$. The values of α and β are found as before, and the results are displayed in figures 5 and 6.

Discussion of solutions

Case $\delta = 0$. We begin our discussion of the solutions with the case $\delta = 0$, which is of particular interest because it is the case for which we already have instability criteria, obtained in § 2 directly by a small perturbation analysis. Figure 3 shows the solutions of (8) in the $-\alpha, \beta$ plane for $\delta = 0$. This consists of, first, the solution $y(x) \equiv 1$, which results when $\alpha + \beta = 0$ and is represented by the straight line OL. Instability of this profile occurs at points where other equilibria bifurcate from the straight line. These are obtained by small perturbations of (8). If (α_0, β_0) is a point on OL at which a bifurcation occurs, let $\alpha = \alpha_0 + \lambda_1$, $\beta = \beta_0 + \mu_1$ and $y(x) = 1 + \zeta_1(x)$, where $\alpha_0 + \beta_0 = 0$, and λ_1, μ_1 and $\zeta_1(x)$ are small perturbations. The first-order change in (8) yields the linear equation

$$d^2\zeta_1/dx^2 + m^2\zeta_1 = \lambda_1 + \mu_1, \quad \text{where} \quad m^2 = 2\beta_0,$$

and we require $\zeta_1(x) = 0$ at $|x| = 1$. Since

$$\zeta_1(x) = (\lambda_1+\mu_1)/m^2 + A_1\cos mx + B_1\sin mx,$$

the boundary condition requires that $B_1 \sin m = 0$. We take the two possibilities in turn.

(i) If $\sin m = 0$, the first non-zero solution is $m = \pi$. Then

$$\zeta_1 = (\lambda_1+\mu_1)(2\beta_0)^{-1}(1+\cos\pi x) + B_1\sin\pi x.$$

The conservation of volume requires that

$$\int_{-1}^{+1} \zeta\, dx = 0,$$

so that $\lambda_1+\mu_1 = 0$ and $\zeta_1 = B_1\sin\pi x$. This gives the first bifurcation from OL, occurring where $2\beta_0 = -2\alpha_0 = \pi^2$, at the point F in figure 3. To obtain the slope of the bifurcation at F it is necessary to go to the second- and third-order terms, which can be obtained without difficulty. The second-order solution yields the results

$$\zeta_2 = (\beta_0/2\pi^2)\, B_1^2(\cos 2\pi x + \cos\pi x),$$

$$\lambda_1 = \mu_1 = 0, \quad \lambda_2+\mu_2 = -\tfrac{3}{2}\beta_0 B_1^2,$$

where the suffixes denote the appropriate orders of the terms. The third-order solution provides the values of λ_2 and μ_2 separately. We find that $\lambda_2 = \frac{3}{16}\pi^2 B_1^2$ and $\mu_2 = -\frac{15}{16}\pi^2 B_1^2$. Thus, the bifurcation occurs at the angle θ with the $-\alpha$ axis, where $\theta = \tan^{-1}5$, and is also one-sided and below the line OL. The fact that $\lambda_1 = \mu_1 = 0$ and the bifurcation only occurs below the line OL can also be proved by expanding the elliptic integral form of the exact solution, which is given by (10) with $\delta = 0$, in the neighbourhood of the point F in figure 3. This is achieved by setting $b = 1+\epsilon$ and $c = 1-\eta$. We then obtain

$$1+2\epsilon-2\eta = (1-\eta)\,F\left(\frac{\pi}{2}, \left(\frac{\epsilon+\eta}{1+\epsilon}\right)^{\frac{1}{2}}\right) \Big/ E\left(\frac{\pi}{2}, \left(\frac{\epsilon+\eta}{1+\epsilon}\right)^{\frac{1}{2}}\right),$$

which, on using the expansion of the complete elliptic integrals for small ϵ and η, yields the result

$$\delta = \epsilon + \tfrac{1}{2}\epsilon^2 + O(\epsilon^3),$$

giving

$$-\beta/\alpha = \gamma = bc = 1 - \tfrac{3}{2}\epsilon^2 + O(\epsilon^3) < 1,$$

from which the stated conclusions follow.

(ii) When $B_1 = 0$, $\zeta_1 = (\lambda_1+\mu_1)(2\beta_0)^{-1}\{1-\cos mx/\cos m\}$ and the volume conservation condition then requires that $\tan m = m$. The first root of this equation is $m \approx 4{\cdot}49$, which gives the bifurcation point G, where $\beta_0 = -\alpha_0 \approx 10{\cdot}08$. Second-order analysis in this case shows that $5\lambda_1+\mu_1 = 0$. In this case one of the first-order coefficients λ_1 or μ_1 must be assigned to set the scale of the first-order solution and since the scaling can be reversed in sign, this suggests that the symmetric bifurcation points on the line $\alpha+\beta = 0$ for $\delta = 0$ are two-sided and consequently the loci of symmetric solutions can be continued above the line $\alpha+\beta = 0$ in figure 3. The fact that bifurcation occurs above and below the line OL for profile types $\lambda+s$ and $\lambda+r$ respectively and the fact that $\lambda_1 \neq \mu_1 \neq 0$ although

the slope of the bifurcation curve is the same as in type (i) can be deduced by expanding the exact solution about the point G in figure 3. We again write $b = 1+\epsilon$ and $c = 1-\eta$ in the equations for the profiles and expand the elliptic integrals up to second order in ϵ and η. Then, on considering $-\beta/\alpha = \gamma = bc$, as in type (i), to see when $\gamma = 1+\epsilon-\eta-\epsilon\eta \gtrless 1$, we find that $\epsilon < \eta$ for the solution $\lambda+r$, implying that $\gamma < 1$, so that this solution bifurcates from the line $\alpha+\beta = 0$ from below while for the solution $\lambda+s$, $\epsilon > \eta$, so that $\gamma > 1$ and hence the bifurcation from $\alpha+\beta = 0$ occurs from above.

Such bifurcation points however have no great physical significance as they do not determine the first onset of instability when $\delta = 0$, and we have not pursued the determination of the $\lambda+s$ curve above the line OL. But the bifurcation branch GN in figure 3 corresponding to the $\lambda+r$ curve for which $\lambda_1 > 0$ and $\mu_1 < 0$ has been calculated and is included in the results displayed in figures 5 and 6, since it is of value in correlating the loci for $\delta = 0$ with those for $\delta \neq 0$. The two bifurcations (i) and (ii) are the first two bifurcations on OL, and they correspond exactly to the sausage modes given by (4) in the limit of large holes, when $kh \to 0$, with $ka = \pi$ and 4·49 respectively.

The loci of bifurcated solutions can be followed in the α, β plane by the direct calculation procedures previously described. In figure 3 they are continued down to the $\beta = 0$ axis. The limiting form of the solutions when $\beta \to 0$ can easily be deduced. When β is small the last term in (8) will only become significant when y becomes very small. It follows that the limiting solutions are sections of parabolas satisfying the equation $d^2y/dx^2 = \alpha$, one parabola joining with another only at a point of discontinuity of slope when $y = 0$. By applying the volume conservation condition in the limit we are able to obtain simply the value of α at which these loci reach the axis $\beta = 0$ for any given δ. For example, the bifurcating curves at F and G for $\delta = 0$ reach the axis at M and N, where $\alpha = -3$ and -6, respectively. FM is clearly a line of asymmetric whole wavelength solutions, whilst GN represents symmetric solutions. The limiting solutions $y(x)$ at M and N are illustrated in figure 4.

Case $\delta \neq 0$. The pattern of solutions in the α, β plane for $\delta = 0$, apart from indicating that instability is associated with bifurcation in the α, β plane, does not advance our knowledge of the stability of fully filled large plane holes, because criteria for instability were obtained in §2 by direct perturbation methods. However, the former method may be followed through for cases in which $\delta \neq 0$, to yield stability criteria which could only be obtained by entirely numerical calculations of stability using the direct perturbation method of §2. In figures 5 and 6 we give results for the loci of equilibria for values of δ less than and greater than zero, respectively, with the case $\delta = 0$ added in each figure for comparison purposes.

For the limiting solutions as $\beta \to 0$ simple calculations show that for asymmetric solutions of the form M, $\alpha = -\frac{3}{2}(\delta+2)$, with the cusp occurring at the point x_0, where $x_0^2 = (3\delta+2)/3(\delta+2)$. For symmetric solutions of the form N we find $\alpha = -6(1+\delta)$. For the value $\delta = -\frac{2}{3}$, $x_0 = 0$, and M corresponds to a symmetric solution and coincides with N. For $\delta < -\frac{2}{3}$ no solution of the form M exists. In this case it can be seen that the point M becomes a second bifurcation point occur-

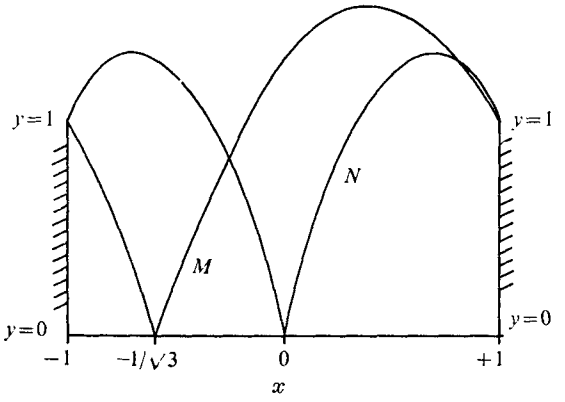

FIGURE 4. The limiting forms of the profiles for $\delta = 0$ as $\beta \to 0$ along the curves FM and GN of figure 3.

ring for $\beta > 0$, at which the λ solution line FM rejoins the symmetric solution $\lambda + r$.

The study of these solutions down to the limit $\beta = 0$ is of interest in establishing the complete pattern of solutions to the mathematical problem posed. However, such solutions near $\beta = 0$ will not have any physical validity because the sharply varying slope near $y = 0$ violates the physical approximation on which the formulation of (8) is based.

4. Breakdown of stable equilibria

In the previous section detailed solutions were obtained for the equilibrium of partially filled two-dimensional large holes when electrically stressed, by use of the Taylor approximation. From a physical point of view we are interested in the stability of the equilibrium, and, in particular, the values of β at which stable equilibrium first fails as β is raised from zero. Starting from $\beta = 0$, the solutions r for $\delta > 0$, and s for $\delta < 0$ represent stable equilibria. As β is raised from zero, stability of the equilibrium for given δ will fail either when a bifurcation point occurs or when the equilibrium locus attains a local maximum in β. It can be seen in figures 5 and 6 that both forms of failure can occur for different values of δ. When $\delta = 0$, the equilibrium first becomes unstable at the bifurcation point F of figure 3, where the instability is of the $S1$ type obtainable from the small perturbation analysis of §2. This type of failure occurs for all $\delta > 0$, and for all negative δ down to a critical value which by numerical methods we find to be about $-0{\cdot}5$. For values of δ which are such that $-\frac{4}{3} < \delta < -\frac{1}{2}$, our results suggest that stable equilibrium remains until β reaches a maximum, which occurs before a bifurcation, and that the stability fails at the maximum point. This happens for example when $\delta = -0{\cdot}67$, as illustrated in figure 7. The lower limit to the range of permissible negative values of δ is imposed by the requirement that $y \geqslant 0$ in the absence of the electric field. The instability of the system represents in practice a rupture of the fluid insulation of the hole, and the two forms of instability represent different forms of rupture. The bifurcation-point instability

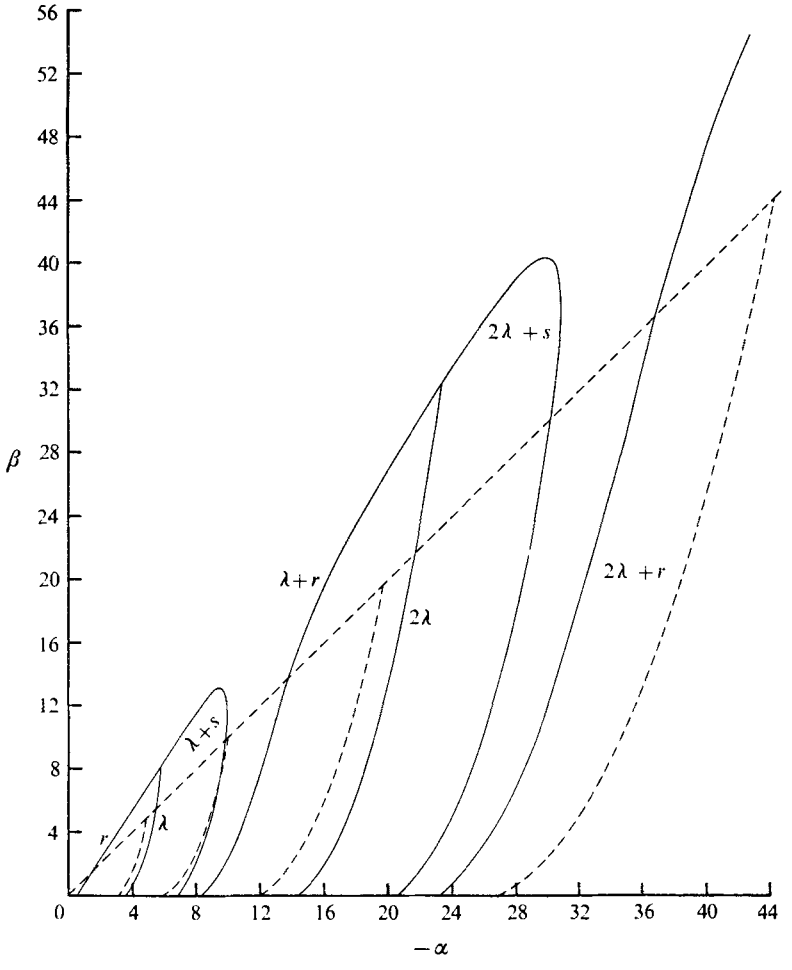

FIGURE 5. β *vs.* α for the solutions of (8) when $\delta = 0{\cdot}4$.

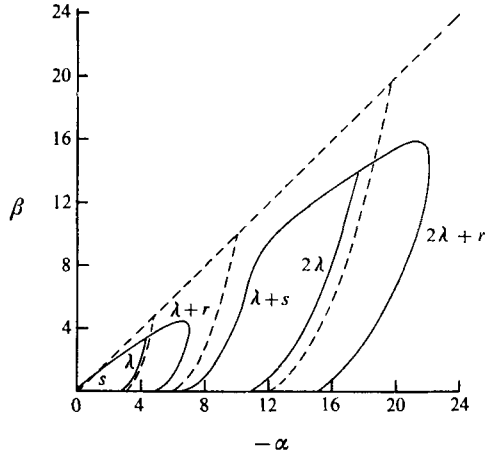

FIGURE 6. β *vs.* α for the solutions of (8) when $\delta = -0{\cdot}2$.

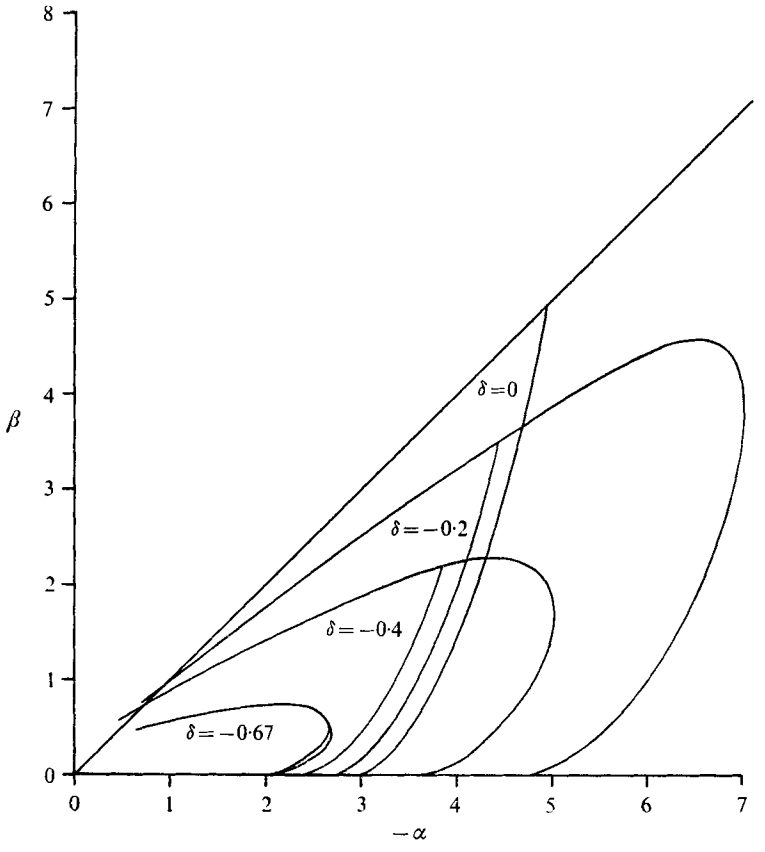

FIGURE 7. β *vs.* α for the solutions of (8) when $\delta = 0, -0{\cdot}2, -0{\cdot}4$ and $-0{\cdot}67$.

$S1$ represents an off-centre rupture of the dielectric fluid and is analogous to the form observed in the experiments of Zuercher for large circular holes, and has up to now been the type of instability associated with large holes. The instability occurring at a maximum of β is symmetric and one in which the rupture occurs at the centre of the hole. Our results indicate that this latter type of instability never occurs when $\delta \geqslant 0$ but will occur for sufficiently large deficiencies in the volume of insulating fluid filling the hole. This may well be expected since in such cases the layer of fluid becomes increasingly thin at the centre as δ decreases. In fact, when $\delta = -0{\cdot}5$, the thickness of the layer at the centre in the absence of the field is $1{\cdot}25h$.

The result of most practical interest is the variation of the critical value of β, denoted by β^*, at which instability first occurs, as a function of δ. For the range of values of δ in which β^* occurs at a bifurcation in the α, β plane, a direct representation of the critical point can be obtained. When $\delta > 0$, $c = 1$ at this point, and if $\alpha = \alpha^*$ and $b = b^*$ at this point, (12) and (13) become

$$2(-\alpha^*)^{\frac{1}{2}} = 2(2b^*)^{\frac{1}{2}} E(\tfrac{1}{2}\pi, (1 - 1/b^*)^{\frac{1}{2}}) \tag{14}$$

and

$$2b^* - 1 - \tfrac{3}{2}\delta = F(\tfrac{1}{2}\pi, (1 - 1/b^*)^{\frac{1}{2}})/E(\tfrac{1}{2}\pi, (1 - 1/b^*)^{\frac{1}{2}}). \tag{15}$$

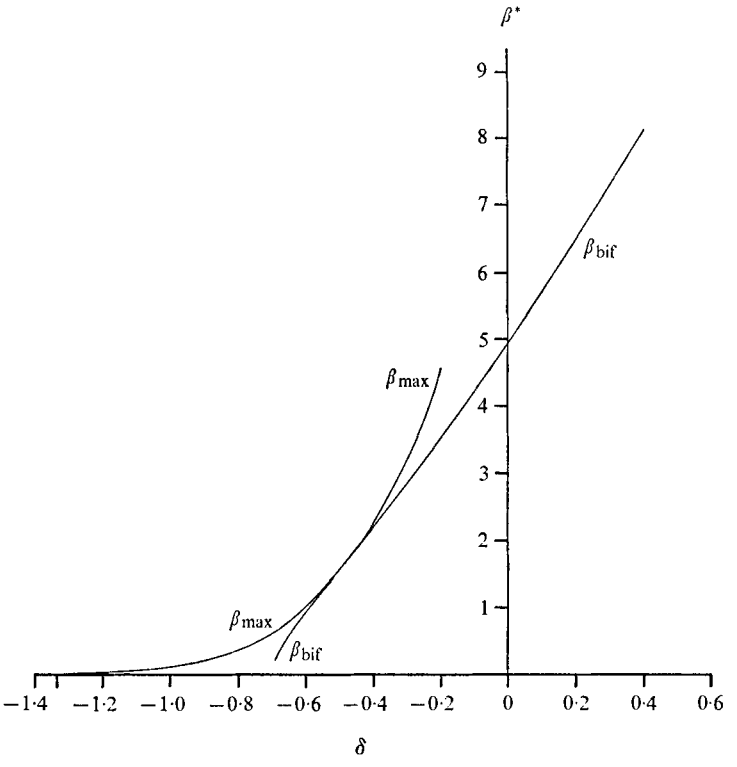

FIGURE 8. A plot of β^*, the value of β in the marginal state of equilibrium, for varying δ. $\beta_{\max}$ denotes the maximum of the α, β locus for symmetric profiles, and β_{bif} denotes the value of β at the first bifurcation of the symmetric and asymmetric loci. The critical value $\beta^* = \beta_{\max}$ for $\delta < -0{\cdot}5$ approximately, and $\beta^* = \beta_{\text{bif}}$ for $\delta > -0{\cdot}5$.

Equation (15) can be solved for b^*. Hence α^* is obtained from (14), and $\beta^* = -\alpha^* b^*$. The function $F(\frac{1}{2}\pi, (1-1/b^*)^{\frac{1}{2}})/E(\frac{1}{2}\pi, (1-1/b^*)^{\frac{1}{2}})$ increases monotonically from 1 to $+\infty$ logarithmically as b^* increases from 1 to $+\infty$. It follows from (15) that for $\delta > 0$ there is just one such bifurcation point of solution r as illustrated in figure 5.

When $\delta < 0$, bifurcation of the solution s occurs where $b = 1$. Equation (15) is then replaced by

$$2c^* - 1 - \tfrac{3}{2}\delta = c^* F(\tfrac{1}{2}\pi, (1-c^*)^{\frac{1}{2}})/E(\tfrac{1}{2}\pi, (1-c^*)^{\frac{1}{2}}), \tag{16}$$

which is solved for c^*, where $0 \leqslant c^* < 1$. It follows from (16) that when $0 > \delta > -\frac{2}{3}$ there is again only one solution for c^*. When $\delta = -\frac{2}{3}$ there is a solution where $F(\frac{1}{2}\pi, (1-c^*)^{\frac{1}{2}})/E(\frac{1}{2}\pi, (1-c^*)^{\frac{1}{2}}) = 2$, for which $0 < c^* < 1$. In addition $c^* = 0$ is a solution giving $\beta^* = 0$. This is the limiting form of a second solution which occurs for values of δ just less than $-\frac{2}{3}$, and is consistent with the behaviour remarked on earlier, that when $\delta < -\frac{2}{3}$ the points represented by M for $\delta = 0$ in figure 3 become bifurcation points of the solutions λ and $\lambda + s$.

At $\delta = \delta_0$, where $-0{\cdot}69 > \delta_0 > -0{\cdot}70$, the points of bifurcation into s and λ, and λ and $\lambda + r$ coalesce, and for $\delta < \delta_0$ these bifurcations no longer exist.

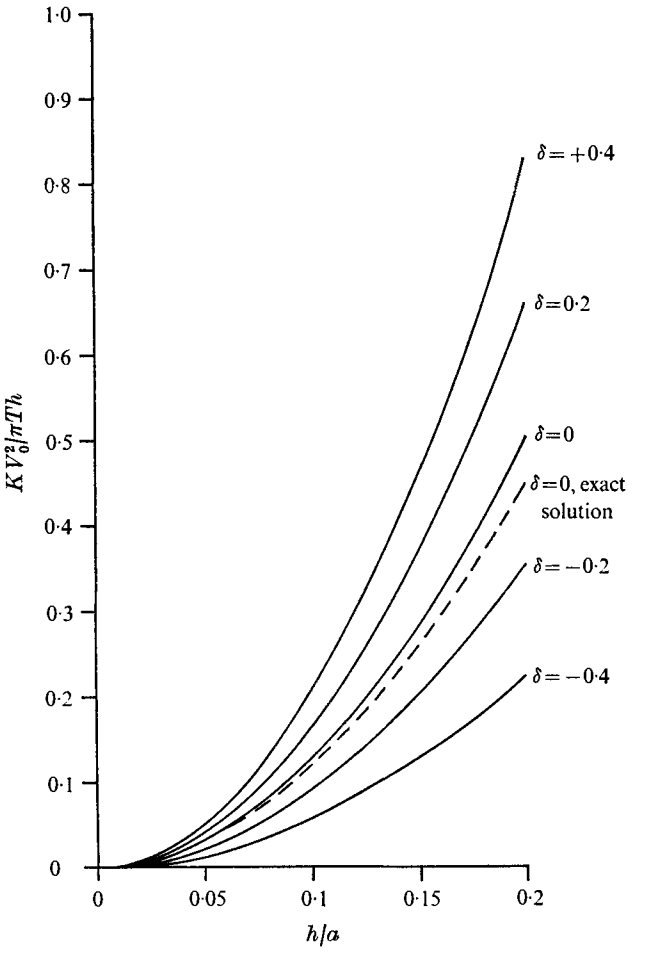

FIGURE 9. $KV_0^2/\pi^2 Th$ *vs.* h/a for fixed values of δ when h/a is small. ---, determined from the exact solution of the linearized perturbation equations when $\delta = 0$ by Miss A. E. Latham (1973; private communication); ——, determined from the present theory.

The determination of the values of β^* occurring where β has a maximum value does not appear to yield to a simple direct analysis of the above type. Maximum points have been obtained in this case by direct evaluation of the s locus for values of δ down to the lower limit $\delta = -\frac{4}{3}$ (where $b^* = 0$) in the neighbourhood of maximum points. Numerical evaluation shows that the critical value of δ at which transition in β^* from a maximum to a bifurcation type occurs is given by $\delta^* = -0{\cdot}5$. The values of β^* are plotted against δ in figure 8.

It is also of interest to correlate these results with those obtained from the small perturbation analysis of §2, and figure 9 shows the critical values of $\lambda^* = 2\pi hT/KV_0^2$ as a function of a/h when $\delta = 0$ for the $S1$ mode. Since $\lambda^* = (4\beta^*)^{-1}(a/h)^2$, we are able to add parabolas obtained here for different values of δ using the value β^* corresponding to each δ. These curves will clearly provide a valid extension of the results of the analysis of §2 when $h/a \ll 1$ and $\delta \neq 0$.

5. Conclusion

In the preceding sections we have demonstrated how the nature of the stability of a fixed volume of incompressible dielectric fluid, which fills a channel between solid dielectric sheets and which is stressed by an electric field applied between the interfaces of the dielectric fluid and conducting fluids, is elucidated by a study of the general problem when the channel is not exactly filled by the dielectric fluid.

In the case when the width of the channel is large compared with its depth, we have shown how an asymmetric rupture of the dielectric fluid results when the curves of potential difference *vs.* pressure difference across the interfaces for symmetric and asymmetric equilibrium profiles of the interfaces bifurcate. This is the mechanism for dielectric breakdown though electrocapillary instability except when the volume of the fluid is less than about half the volume of the channel per unit length, and in such cases, the rupture of the dielectric fluid occurs at the centre and the critical field then corresponds to the maximum in the curve of potential difference *vs.* pressure difference for symmetric equilibrium profiles. It has also been established that bifurcations only occur when the equilibrium profiles of the interfaces have extrema at the edges of the channel.

The work described in this paper was completed while one of the authors (M. E. O'N.) was visiting the Department of Mathematics, University of Toronto, and he gratefully acknowledges support from the National Research Council of Canada.

REFERENCES

ABRAMOVITZ, M. & STEGUN, I. A. 1965 *Handbook of Mathematical Functions*. Dover.
ACKERBERG, A. 1969 *Proc. Roy. Soc.* A **312**, 129.
BASSETT, A. B. 1894 *Am. J. Math.* **16**, 93.
CROWLEY, J. M. 1965 *Phys. Fluids*, **8**, 1668.
MELCHER, J. R. 1963 *Field Coupled Surface Waves*. M.I.T. Press.
MICHAEL, D. H. & O'NEILL, M. E. 1972*a* *Proc. Roy. Soc.* A **328**, 529.
MICHAEL, D. H. & O'NEILL, M. E. 1972*b* *Phil. Trans.* A **272**, 331.
MICHAEL, D. H., O'NEILL, M. E. & ZUERCHER, J. C. 1971 *J. Fluid Mech.* **47**, 609.
RAYLEIGH, LORD 1879 *Proc. Roy. Soc.* **29**, 406.
TAYLOR, G. I. 1968 *Proc. Roy. Soc.* A **306**, 423.
TAYLOR, G. I. 1969 *Proc. Roy. Soc.* A **313**, 453.
TAYLOR, G. I. & MCEWAN, A. D. 1965 *J. Fluid Mech.* **22**, 1.